JOURNAL OF MODERN OPTICS, 1995, VOL. 42, NO. 2, 483–488

Dynamics of induced lightbeam deflection in an off-axis geometry

A. DREISCHUH, D. KAVALDJIEV and S. DINEV
Department of Physics, Sofia University,
5, J. Bourchier Blvd., 1126 Sofia, Bulgaria

(*Received 28 April 1994; accepted 8 July 1994*)

Abstract. The induced deflection of a probe beam in an off-axis geometry is investigated with respect to its temporal and spatial evolution. A method for picosecond pulse duration measurement is proposed which seems to be especially promising in the UV and XUV region.

1. Introduction

The all-optical control of lightbeam spatial parameters is of increasing importance. The basic phenomena of self-induced, respectively induced focusing originate in the (self)induced refractive index change along/across nonlinear media. It is known that an asymmetrical intensity distribution at the entrance of the nonlinear medium could lead to a beam self-deflection [1–3]. The physical picture becomes more complicated when the interaction takes place between two co-propagating beams with an initial angular deviation and/or off-axial separation. The induced focusing of a probe beam in a self-defocusing medium was proposed in the pioneering paper of Agrawal [4]. The experimental results reported [5] are in a good agreement with the theory. The induced deflection of an optical beam in an off-axis geometry is analysed extensively both theoretically [6, 7] and experimentally [8, 9].

In this work we analyse the spatio–temporal dynamics of the induced deflection (ID) of a probe beam in an off-axis geometry. The temporally integrated transverse intensity distribution of the beam is shown to differ significantly from the distribution obtainable in single-spatial-dimension analyses [10]. The ID can be controlled effectively by the initial delay between the pulses. On this basis, a method for pulse duration measurements is proposed, which seems to be particularly attractive in the short wavelength region as an alternative to multiple-shot correlation and two-photon fluorescence techniques [11].

2. Theoretical analysis

The nonlinear medium considered is taken to be homogeneous and to have a resonant structure (e.g. inert gas). Choosing the pump and probe frequencies ω_p and ω_s near an $\omega_p + \omega_s$ two-photon resonance, ω_p and ω_s being far from single-photon resonances, the beam/pulse self-action should be negligible compared with the induced phase modulation (IPM). In a pump-probe configuration the IPM of the pump originating from the probe beam/pulse should be negligible too, and the pump beam should experience diffraction only. These assumptions are made to retain the possibility of studying the pure effect of ID, although they are not obligatory for observing it experimentally [5].

Under these conditions, in a spatio–temporal coordinate system connected with the pump, the time-dependent paraxial wave equation, describing the signal beam/pulse evolution, has the form

$$\mathrm{i}\left(\frac{\partial}{\partial z}+v_{\mathrm{sp}}\frac{\partial}{\partial t}\right)E_{\mathrm{s}}+\alpha_{\mathrm{s}}\left(\frac{\partial^2}{\partial x^2}+\frac{\partial^2}{\partial y^2}\right)E_{\mathrm{s}}+\alpha_{\mathrm{t}}\frac{\partial^2 E_{\mathrm{s}}}{\partial t^2}+k^{\mathrm{IPM}}(\omega_{\mathrm{s}})|E_{\mathrm{p}}|^2E_{\mathrm{s}}=0, \tag{1}$$

where E_s and E_p are the slowly varying amplitudes of the signal and pump, $v_{sp}=(V_{GS}^{-1}-V_{GP}^{-1})$ and reflects the group velocity mismatch between the probe and pump pulses, $\alpha_s=1/(2k_s)$, k_s is the wavenumber of the probe, α_t is the group velocity dispersion parameter and $k^{\mathrm{IPM}}(\omega_s)=[n_2^{\mathrm{IPM}}(\omega_s)k_s/(2n_0(\omega_s))]$ and is the nonlinear coefficient for IPM. In a planar nonlinear (e.g. gas filled) optical waveguide one can set $\partial^2E_s/\partial y^2=0$. Because of the limited computing resources available, we made the following simplifications:

(i) The probe wave was divided into $4N$ slices, each one having a duration of $\tau_{\mathrm{SLICE}}=\tau_{\mathrm{HW1/e}}/N$. The minimum slice number required ($N=50$) was determined from both the energy conservation and the reproducibility of the transverse intensity distribution in the time-integrated picture against increasing N twice.

(ii) The walk-off length $L_w=\tau_{\mathrm{HW1/e}}/|v_{sp}|$ is assumed to be much larger than the nonlinear medium length L_{NL}. This implies that the initial delay τ_d between the pump and probe pulses remains nearly unchanged by the walk-off effect. This simplification holds until $|v_{sp}|L_{\mathrm{NL}}<\tau_{\mathrm{HW1/e}}/(2N)$.

(iii) The dispersion length $L_{\mathrm{DISP}}=\tau_{\mathrm{HW1/e}}/(2|\alpha_t|)$ for both waves is assumed to be much larger than L_{NL}, which, along with the previous simplifications, determines the conditions under which the results presented are valid.

(iv) As a consequence of the above mentioned assumptions, the initial delay τ_d between the pulses can be introduced adequately if $\tau_d=M\tau_{\mathrm{SLICE}}$, where M is an integer.

We studied the ID of a probe beam/pulse with an initial form

$$E_s\,(x,z=0,t)=E_{s0}\exp\{-(x-x_0)^2/a_s^2\}\exp\{(t-\tau_D)^2/2\tau_s^2\} \tag{2}$$

caused by a co-propagating pump wave of the type

$$E_p\,(x,z=0,t)=E_{p0}\exp\{-x^2/a_p^2\}\exp\{t^2/2\tau_p^2\} \tag{3}$$

where a_s and a_p are the beam radii at the entrance of the nonlinear medium, x_0 is the distance between the beam centres, τ_s and τ_p are the pulse durations of the probe and the pump, respectively, and τ_d is their initial temporal offset. This simple model does not account for the nonlinear evolution of the pump beam, but even under pump beam self-defocusing, this effect could be experimentally compensated for by an initial gentle focusing [2]. Equation (1) was solved using the split-step Fourier method.

3. Discussion

For simplicity of presentation, figure 1 plots the transverse intensity distribution (along the diffraction non-limited coordinate x) over the probe beam cross-section at a distance $L=1$ m from the entrance of the nonlinear medium for $t=2\tau_s$ (curve 1), $t=1{\cdot}2\tau_s$ (curve 2), $t=0{\cdot}4\tau_s$ (curve 3) and $t=0$ (curve 4). Synchronous pulse propagation ($\tau_d=0$) and equal pulse durations are assumed. The choice a_s

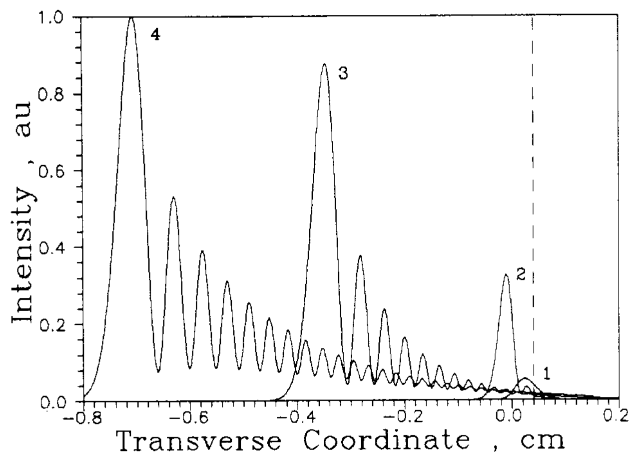

Figure 1. Transverse intensity distributions of the probe beam at $L_{NL} = 6$ cm, $L = 1$ m, $\tau_d = 0$, $a_s(z=0)/a_p = 0{\cdot}4$, $x_0(z=0)/a_p = 0{\cdot}4$, $a_p = 0{\cdot}1$ cm and $\Delta_n = \frac{1}{2}n_2^{IPM}|E_p|^2 = -5 \times 10^{-5}$ at local times $t = 2\tau_s$ (1), $t = 1{\cdot}2\tau_s$ (2), $t = 0{\cdot}4\tau_s$ (3) and $t = 0$ (4).

$(z=0)/a_p = 0{\cdot}4$ and $x_0\,(z=0)/a_p = 0{\cdot}4$, $a_p = 0{\cdot}1$ cm enables a strong ID to be achieved [6] at a nonlinear refractive index correction $\Delta n = \frac{1}{2}n_2^{IPM}|E_p|^2 = -5 \times 10^{-5}$. The dashed line represents the position of the probe beam at the entrance of the nonlinear medium. The oscillatory behaviour of the probe-beam wing is a result of the spatial analogue of optical wave breaking, in agreement with the experimental observations of Stenz *et al.* [5]. Because of the increased pump intensity near the pump pulse peak, the oscillations become stronger for probe beam parts closer to the central part of the pump. This agrees with the analyses in [8, 12], where an intensity-dependent (self)induced deflection combined with a far-field spatial filtering is used for pulse shaping and shortening. The experimental geometry in [5] involves angularly offset beams of coincident centres at the entrance of the nonlinear medium, in contrast to the off-axis geometry analysed here. Nevertheless, the one-dimensional transverse distribution obtained is quite similar to the experimental one (compare curve 2 on figure 1 with figure 2 (*b*) in [5]). A slice, temporally offset from the pump by $t = 1{\cdot}2\tau_p$, has a local intensity $I_p(t = 1{\cdot}2\tau_p) = I_p(t=0)/4$ (curve 2 on figure 1), whereas the intensity where the value of the refractive index correction Δn in [5] is 5 times lower than in the present analysis.

In figure 2 (*a*), the transverse, temporally integrated intensity distributions of the probe beam at $L = 1$ m are shown for different values of the normalized delay $|\tau_d|/\tau_s$. Curve 1 ($\tau_d = 0$) represents the temporally integrated spatial probe beam profile corresponding to the spatio-temporal distributions from figure 1. The comparison is indicative of the difference between the results of the one-transverse-spatial-dimension model and the temporally-integrated picture, which could be recorded experimentally [5]. Curves 2, 3, 4, 5, and 6 correspond to $|\tau_d|/\tau_s = 0{\cdot}4$, $0{\cdot}8$, $1{\cdot}2$, $1{\cdot}6$, and 4, respectively. As seen, the transverse probe beam spreading and the spatial wave breaking become weaker with increasing initial temporal delay $|\tau_d|$. In the limiting case $|\tau_d| \gg \tau_s$ (temporally separated pulses), the probe wave remains undistorted by the pump. The dashed line in figure 2 (*a*) denotes a specific transverse position of the probe beam—the maximum deviated peak in the temporally

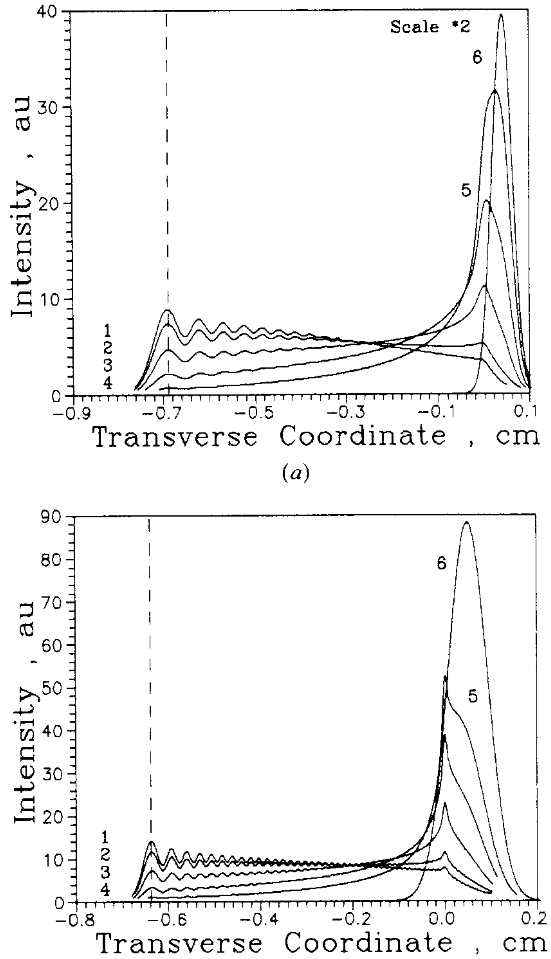

Figure 2. Temporally-integrated probe beam intensity distribution at $L = 1$ m against normalized delays $|\tau_d|/\tau_s = 0$ (1), 0·4 (2), 0·8 (3), 1·2 (4), 1·6 (5), and 4 (6). The model parameters for (*a*) are the same as in figure 1. The corresponding parameters for (*b*) are $L_{NL} = 3$ cm, $L = 1$ m, $a_s(z = 0)/a_p = 0{\cdot}6$, $x_0(z = 0)/a_p = 0{\cdot}5$, $a_p = 0{\cdot}1$ cm and $\Delta_n = \frac{1}{2} n_2^{IPM}|E_p|^2 = -4{\cdot}5 \times 10^{-4}$.

integrated picture at $\tau_d = 0$. One can note that the decrease in the relative intensity of this peak as a function of $|\tau_d|/\tau_s$ does exhibit a monotonic character.

Figure 2 (*b*) plots a similar transverse, temporally integrated picture, numerically generated using $a_s(z = 0)/a_p = 0{\cdot}6$ and $x_0(z = 0)/a_p = 0{\cdot}5$, $a_p = 0{\cdot}1$ cm, $L_{NL} = 3$ cm, $L = 1$ m and $\Delta n = -4{\cdot}5 \times 10^{-4}$. Curve 1 corresponds to $\tau_d = 0$, whereas curves 2, 3, 4, 5 and 6 correspond to $|\tau_d|/\tau_s = 0{\cdot}4$, 0·8, 1·2, 1·6, and 4, respectively. Qualitatively, the characteristic features of these curves are similar to those from figure 2 (*a*). The model parameters are chosen not to correlate with the parameters used in the generation of figure 2 (*a*), but to retain a well expressed effect of ID on the probe beam. The dashed line indicates again the position of the maximum deviated peak of the probe beam at $\tau_d = 0$.

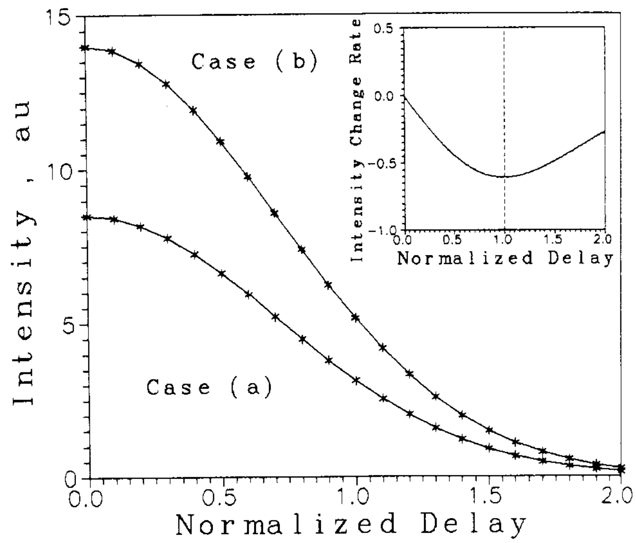

Figure 3. Local intensity at the position of the maximum deviated peak of the probe beam/pulse for $\tau_d = 0$ against normalized delay $|\tau_d|/\tau_s$. Case (*a*) corresponds to figure 2 (*a*); Case (*b*) corresponds to figure 2 (*b*). The solid lines are Gaussian fits (see equation 4). The insert shows the pump intensity change rate against $|\tau_d|/\tau_p$.

From a practical point of view, this position seems to be of particular importance. Further, let us concentrate our analysis on the dependence of its local intensity on the initial pulse delay $|\tau_d|$, plotted in figure 3. The points are extracted from figure 2 (*a*) and figure 2 (*b*), respectively, and represent the intensity I_M at the position of the maximum deviated peak (at $\tau_d = 0$) as a function of the normalized delay $|\tau_d|/\tau_s$. As shown theoretically in our previous analysis [13], the effective nonlinearity $\tilde{k}^{IPM}$ depends on the pulse durations and τ_d according to

$$\tilde{k}^{IPM} = k^{IPM} \exp\{-\tau_d^2/(\tau_s^2 + \tau_p^2)\} = k^{IPM} T(\tau_s, \tau_p, \tau_d). \qquad (4)$$

The solid lines in figure 3 are Gaussian fits (equation 4) of the theoretically predicted values, obtained by solving equation 1, the function $T(\tau_s, \tau_p, \tau_d)$ being normalized to the corresponding peak. It is natural to expect that the maximum intensity change rate (at this specific position) vs. $|\tau_d|$ corresponds to the maximum change rate of $\tilde{k}^{IPM}$ (i.e. of $T(\tau_s, \tau_p, \tau_d)$) and takes place at

$$2\tau_{d_M}^2 = \tau_s^2 + \tau_p^2. \qquad (5)$$

Assuming equal pump and probe pulse durations $\tau_s = \tau_p = \tau$, equation 5 is transformed into $|\tau_{d_M}|/\tau = 1$. The insert on figure 3 plots the local intensity change rate at the position of the maximum deviated peak at $\tau_d = 0$ versus normalized delay, $|\tau_d|/\tau_s$. This dependence has a minimum (i.e. a maximum if absolute values are considered) at $|\tau_d|/\tau_s = 1$, which agrees with equation 5.

Based on this analysis, one can propose an approach for pulse duration measurements in a configuration in which the pump and probe waves co-propagate in a nonlinear medium with an initial off-axis separation. Recording the temporally integrated intensity distribution of the probe beam over the diffraction non-limited transverse coordinate, one can obtain experimentally the dependence $I_M(|\tau_d|/\tau_s)$ at the position of the maximum deviated peak at $\tau_d = 0$. From the maximum change rate of $I_M(|\tau_d|/\tau_s)$, using equation 5, it is easy to deduce the pulse durations. In the case of different pulse durations, one of them should be known in order to measure the duration of the other one.

This technique seems particularly attractive in the short wavelength spectral region. As an example, figure 2 (*a*) corresponds to pump and probe wavelengths $\lambda_p = 248$ nm and $\lambda_s = 264{\cdot}42$ nm, respectively, and the inert gas Xe (1 atm) as a nonlinear medium (resonance $5p^6 - 6p[5/2]_2$). Figure 2 (*b*) corresponds to $\lambda_p = 650$ nm, $\lambda_s = 121{\cdot}6$ nm (Ly-α-line of the H atom), and Kr (1 atm) as a nonlinear medium (resonance $4p^6 - 5p[3/2]_1$). It is important to evaluate the minimum pulse duration measurable with this technique. We believe that this approach should be applicable even in the subpicosecond range. Because of the simplifications made in our numerical procedure (especially points (ii) and (iii)), the calculated values of the group velocity mismatch parameter $v_{sp}(|v_{sp}| = 1{\cdot}8 \times 10^{-2}$ ps cm^{-1} for figure 2 (*a*) and $6{\cdot}4$ ps cm^{-1} for figure 2 (*b*)) imply, that pulse durations down to 5 ps and 1 ns, respectively, could be adequately measured. It should be pointed out that these limitations are not the physical limits of the technique proposed and rather are posed by the simplified computing procedure used.

4. Conclusion

In conclusion, we have studied the spatio-temporal dynamics of the induced probe beam deflection in an off-axis geometry. The temporally integrated transverse intensity distributions obtained numerically are in a good qualitative agreement with the experimental results of other authors. An approach for pulse duration measurement is proposed, potentially applicable in the short wavelength and subpicosecond spectral/temporal region.

Acknowledgment

This work was done with the financial support of the National Foundation 'Young Scientist', Bulgaria, under contract No. MU-TT-1/1991.

References

[1] Kaplan, A., 1969, *JETP Lett.*, **9**, 3.
[2] Borodin, M. S., and Kamuz, A. M., 1969, *JETP Lett.*, **9**, 351.
[3] Swartzlander, Jr., G., Yui, H., and Kaplan, A., 1989, *J. opt. Soc. Am.* B, **6**, 1317.
[4] Agrawal, G. P., 1990, *Phys. Rev. Lett.*, **64**, 2487.
[5] Stenz, A. J., Kauranen, M., Maki, J. J., Agrawal, G. P., and Boyd, R., 1992, *Optics Lett.*, **17**, 19.
[6] Dinev, S., Dreischuh, A., and Ivanova, I., 1992, *J. mod. Optics*, **39**, 667.
[7] Dinev, S., Dreischuh, A., and Ivanova, I., 1993, *Appl. Phys.* B, **56**, 34.
[8] Barthelemy, A., Froehly, C., Maneuf, F., and Reynaud, F., 1992, *Optics Lett.*, **17**, 844.
[9] Golub, I., 1992, *Optics Commun.*, **94**, 143.
[10] Aitchison, J. S., Silberberg, Y., Weiner, A. M., Leaird, D. E., Oliver, M. K., Jackel, J. L., Vogel, E. M., and Smith, P. W. E., 1991, *J. opt. Soc. Am.* B, **8**, 1290.
[11] Tünnermann, A., Eichmann, H., Henking, R., Mossavi, K., and Wellegehausen, B., 1991, *Optics Lett.*, **16**, 402.
[12] Dreischuh, A., Eugenieva, E., and Dinev, S., 1994, *IEEE J. Quant. Electron.*, **30**, 1656.
[13] Blagoeva, A., Dinev, S., Dreischuh, A., and Naidenov, A., 1991, *IEEE J. Quant. Electron.*, **27**, 2060.